Available online at www.sciencedirect.com
SCIENCE DIRECT®
Polymer 45 (2004) 3765–3779
polymer
www.elsevier.com/locate/polymer

Mechanical properties of polyketone terpolymer/rubber blends

W.C.J. Zuiderduin*, D.P.N. Vlasveld, J. Huétink, R.J. Gaymans

Department of Chemical Technology, University of Twente, P.O. Box 217, 7500 AE Enschede, The Netherlands

Received 17 November 2003; received in revised form 15 March 2004; accepted 23 March 2004

Abstract

Blends of aliphatic polyketone terpolymer and a core-shell rubber (CSR) were melt processed with varying CSR concentration of 0–40 wt%. The obtained morphology was of finely dispersed CSR particles in the polyketone matrix. The thermal properties of the matrix polymer remained unaffected by the addition of the CSR phase. The crystallinity remained constant at 35 wt% and the melting temperature was not changed. The tensile modulus and yield stress were decreased by the addition of the rubber phase to the aliphatic polyketone polymer. The deformation was strongly delocalised with increasing CSR content. The temperature development during fracture was also strongly reduced with increasing rubber concentration. The CSR phase was found to toughen the aliphatic polyketone matrix very effectively, the brittle to ductile transition temperature was lowered from 90 to −40 °C with the highest rubber concentration (40 wt%). Cavitation experiments revealed that the macroscopic cavitation strain remained constant with increasing rubber content. A study of the deformation zone below the fracture surface showed that voids were produced by cavitation of the rubber phase. The voids were strongly deformed by the plastic deformation of the matrix polymer. At high strain rates a relaxation layer was found below the fracture surface, where the voids were no longer present. This relaxation zone was found to be due to the adiabatic temperature rise of the material during fracture at high strain rates.

Keywords: Impact; Tensile properties; Toughness

1. Introduction

The aliphatic polyketones studied are semi-crystalline polymers with a glass transition temperature of approximately 15 °C and a melting temperature of 225 °C. The starting materials of polyketones are relatively cheap, carbon monoxide, ethylene and propylene. Aliphatic polyketones possess excellent properties like fast crystallisation, high tensile strength, high chemical and wear resistance, very low permeability and good impact behaviour over a broad temperature range [1,2]. These properties make polyketone a suitable material for engineering applications. Unnotched samples of semi-crystalline polymers often fracture in a ductile manner. However, with a notch or defect they nearly all show brittle fracture [3]. Semi-crystalline thermoplastics are often toughened with a rubber phase.

It is now well accepted that the role of the rubber phase is to cavitate and thereby change the stress state of the matrix material in the neighbourhood of the cavitated particle [4–7]. The stress state is changed from a plane strain state behind the notch tip towards the direction of a plane stress state. In this situation, the sensitivity towards crazing is reduced significantly and shear yielding of the matrix polymer becomes favourable [8]. The cavitation process is possible when a volume strain is applied to the rubber particle. This volume strain stems from the tri-axial stress state ahead of the notch tip.

The elastic energy that is stored in the system is released by cavitation and the tri-axial stress state is converted towards a biaxial one. Both the cavitation and the deformation of the matrix polymer dissipate energy, but the mechanism that consumes the most energy is shear yielding of the matrix [9,10].

Important aspects that influence cavitation are the size of the rubber particles and the adhesion of these particles to the matrix polymer [8]. Particles larger then 1 μm generally lead towards crazing [11]. Multiple crazing only is effective in HIPS, but this mechanism is usually not favourable in semi-crystalline polymers. As a general rule, brittle glassy matrices that tend to craze benefit more from large rubber

* Corresponding author. Tel.: +31-534894347; fax: +31-534893823.
E-mail address: w.c.j.zuiderduin@ct.utwente.nl (W.C.J. Zuiderduin).

0032-3861/$ - see front matter © 2004 Elsevier Ltd. All rights reserved.
doi:10.1016/j.polymer.2004.03.080

Table 1
Material properties

Material	Produced by	Description
Polyketone terpolymer: Carilon P1000	SHELL Research and Technology Centre Amsterdam	Polyketone terpolymer with 6 mol% propylene. Density 1.24 g/cm^3. T_m : 225 °C, T_g : 15°.
Rubber phase: Blendex 338	GE plastics	Core-shell rubber (CSR), Polybutadiene (PB) core with a Styrene-acrylonitrile shell: Particle size: 0.7 μm, 70% PB content, density 0.95 g/cm^3.

particle size, i.e. in excess of 1 μm. On the other hand, matrices that can absorb fracture energy via shear yielding are effectively toughened with relative small particle size modifiers, on the order of 0.5 μm and less [11].

An effective way to guaranty a uniform particle size distribution and to create sufficient adhesion between the particles and the matrix polymer, is the use of core-shell modifiers. A major distinction between core-shell particles and other types of impact modifiers is that their size is set during the synthesis and remains the same after they are dispersed into the host matrix polymer [12,13].

The particles used in this paper are core shell particles with a diameter of 0.7 μm. Cavitation should not occur too early in the process since blends with cavitated particles have a higher creep rate [14]. The creation of free volume at the particle size level must occur prior to the yield strain of the matrix polymer. Just in time cavitation is what is desirable. Relieving the volume strain by cavitation is directly related to the rubber content [15] and also the stress concentration is directly related to the rubber content [4]. The morphology of the semi-crystalline polymer can be affected by the dispersed rubber phase. The rubber particles may disturb the formation of the spherulitic structure [16,17]. However, the crystallinity is usually not at all, or in some cases only slightly, affected by the introduction of a rubber phase [18–20].

Deformation and impact behaviour of semi-crystalline polymers has been studied extensively [5,6,21–26]. The modulus as well as the yield stress decrease with rubber content. This decrease exceeds the expectations based on the rule of mixtures. The particle size has no or only slightly effect on the modulus and yield stress of the blend [27]. The notched fracture behaviour of polyketone terpolymers depends on the temperature as well as the strain rate [28]. An important feature of fracture behaviour of polymers is the discontinuous transition from brittle to ductile fracture. An increase in rubber content decreases the brittle-to-ductile transition temperature linearly [29], as well as a linear decrease of the yield stress [30].

Even though the particle size of core-shell polymers is fixed during the emulsion process; proper dispersion in the melt must be achieved to obtain optimum toughening performance. Kayano et al. [31] have shown that better dispersion translated into higher notch Izod impact strength and a lower brittle-to-ductile transition [32,33].

There have been a number of papers on the subject of aliphatic polyketones, especially the crystallisation behaviour and crystal structure have been a subject of interest [34–37], however, to our knowledge no papers have been reported that deal with rubber toughening of aliphatic polyketone terpolymers.

1.1. Aim

The aim is to study the impact behaviour of polyketone terpolymer toughened with a core-shell rubber phase (CSR) as a function of CSR content. The cavitation behaviour of the rubber will be investigated and also the micro fracture mechanism will be investigated by means of electron microscopy. The mechanical and thermal properties of the polymer-rubber system are studied as a function of CSR content.

2. Experimental

2.1. Materials

SHELL and GE Plastics kindly supplied commercially available polyketone and Blendex core-shell rubber. Material specifications are listed in Table 1. The polyketone used here is a perfect alternating terpolymer, polymerised from ethylene and carbon monoxide; 6 mol% of the ethylene is replaced by propylene compared to PK-E to lower the melting temperature. This polyketone has a glass transition temperature of approximately 15 °C and a melting temperature of 225 °C with a crystallinity of 35 wt%.

2.2. Specimen preparation

Blends were prepared from polyketone terpolymer and the CSR particles. Blend composition was varied between 0 and 40 wt%. Compounding of the materials was done using a Berstorff (ZE 25 × 33D) twin screw (co-rotating) extruder. In the extrusion step, barrel temperatures were set at 225/240/240/240/240/240/240 °C and a screw speed of 140 rpm with a throughput of 4 kg/h. The L/D ratio of the screws was 33, and $D = 25$ mm. The raw materials were fed in the middle section of the extruder to reduce residence time. A nitrogen flow was maintained over the extruder to

Table 2
Technical data for the infrared camera, equipped with close-up lens

TVS 600 AVIO Nippon Avionics Co.	
Temperature range	−20–300 °C
Temperature resolution	0.15 °C
Spectral range	8–14 μm
Image rate	30 frames/s
Spatial resolution	0.1 mm spot size

avoid oxidation of the polymer. During the extrusion process stabilisers were added, 0.2 wt% calcium-hydroxy-apatite (melt stabilisation), 0.3 wt% Nucrel (ethylene-methacrylic acid copolymer, processing aid) and 0.2 wt% Naugard (2-2′-oxamidobis(ethyl-3(3,5 di-t-butyl-4-hydro-xyphenyl)propionate), anti oxidant).

The polymer was injection moulded into rectangular bars (74 × 10 × 4 mm) impact test specimen and Dumbbell shaped specimen using an Arburg Allrounder 221-55-250 injection moulding machine.

The barrel had a flat temperature profile of 20 °C above the melt temperature (T_m + 20 °C), the mould temperature was kept at 70 °C with an injection pressure of 55 bar, holding pressure was kept at 45 bar. Total cycle time was approximately 23 s.

A single-edge V-shaped notch of 2 mm depth and tip radius 0.25 mm was milled in the moulded specimens for the notched Izod impact test.

2.3. Conditioning

The test bars were dried at 80 °C under vacuum for 15 h, and kept under vacuum at room temperature after this drying step. Although physical ageing generally refers to a relaxation process of the amorphous phase below its glass transition temperature, semi-crystalline polymers may also show ageing at temperatures slightly above the glass transition temperature [38] due to amorphous regions with restricted mobility. This ageing affects the stiffness of the polymer and also influences the mechanical properties. Because of this physical ageing behaviour of this type of polyketone terpolymers, every 10th day the test bars were heated to 80 °C for half an hour to rejuvenate the physical ageing. After this treatment the test bars were cooled down in a controlled manner in the oven and kept under vacuum. The test bars are not used in the first two days after a heat treatment since the physical ageing process is very fast in this period. This thermal rejuvenation did not effect the crystallinity of the material as measured by differential scanning calorimetry.

2.4. Scanning electron microscopy (SEM)

SEM pictures were taken to study the morphology of the rubber blends. Samples were taken from the core of the injection moulded bars. SEM specimens were prepared by cutting with a CryoNova microtome at −120 °C using a diamond knife (−110 °C) and cutting speed of 1 mm/s. The cut surfaces were then sputter-coated with a thin gold layer and studied with Hitachi S-800 field emission SEM.

2.5. Notched Izod impact test

Notched Izod impact tests were carried out using a Zwick pendulum according to ISO 180. To vary the test temperature, the specimens were placed in a thermostatic bath. The impact strength was calculated by dividing the absorbed energy by the initial cross-sectional area behind the notch (32 mm^2). All measurements were carried out in ten-fold.

2.6. DSC

DSC spectra were recorded on a Perkin Elmer DSC7 apparatus, equipped with a PE7700 computer and Tas-7 software. 2–5 mg of dried sample was heated at a rate of 20 K/min. The peak temperature of the second scan was taken as the melting temperature of the polymer; the peak area was used to determine the enthalpy.

2.7. Tensile tests

Standard tensile tests were conducted on dumbbell shaped specimens with a Zwick tensile tester type ZO2, all tests were carried out in five folds. Extensometers were used to measure the strain during the tensile test. Test speed was kept at 60 mm/min. During the test the force was recorded versus nominal strain.

2.8. Infrared thermography

The temperature rise during fracture of specimens of thickness 4 mm was monitored using an infrared camera. Camera specifications are listed in Table 2. With the infrared camera, only temperatures at the surface of the specimen can be determined. The spot size of about 100 μm is relatively large. The temperature indicated in one spot is an average temperature over the entire spot size. The temperature can therefore not be determined directly at the fracture surface, which is expected to be highest.

In high speed tests only the temperature of an already broken specimen can be determined.

2.9. Onset of cavitation of rubber particles in a matrix polymer

The cavitation measurements were performed on a Schenck hydropulse 25 VHS high speed hydraulic tensile tester. The laser used was a helium–neon laser with a maximum output power of 30 mW and a wavelength of 633 nm. The data were sampled using a transient data

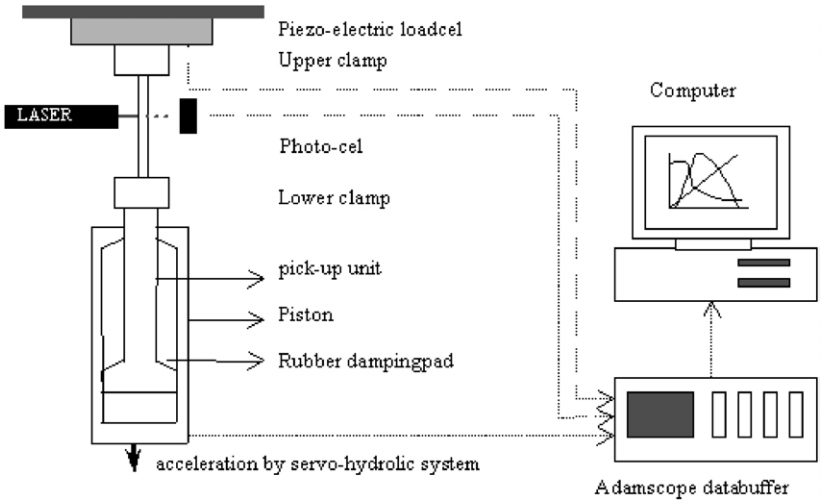

Fig. 1. Test set-up for measuring the onset of cavitation of rubber particles in a matrix polymer.

recorder after which the data was transferred to a computer set-up. The test set-up is given in Fig. 1.

The principle of the method is that cavitation in a blend is accompanied by a change in transparency due to stress whitening. The stress whitening is caused by the scattering of the incident light by cavitated particles. When a strong light source is positioned on one side of the specimen, it is expected that at the onset of cavitation the intensity of the transmitted light will drop suddenly. This lowering of the intensity of transmitted light can be detected by a

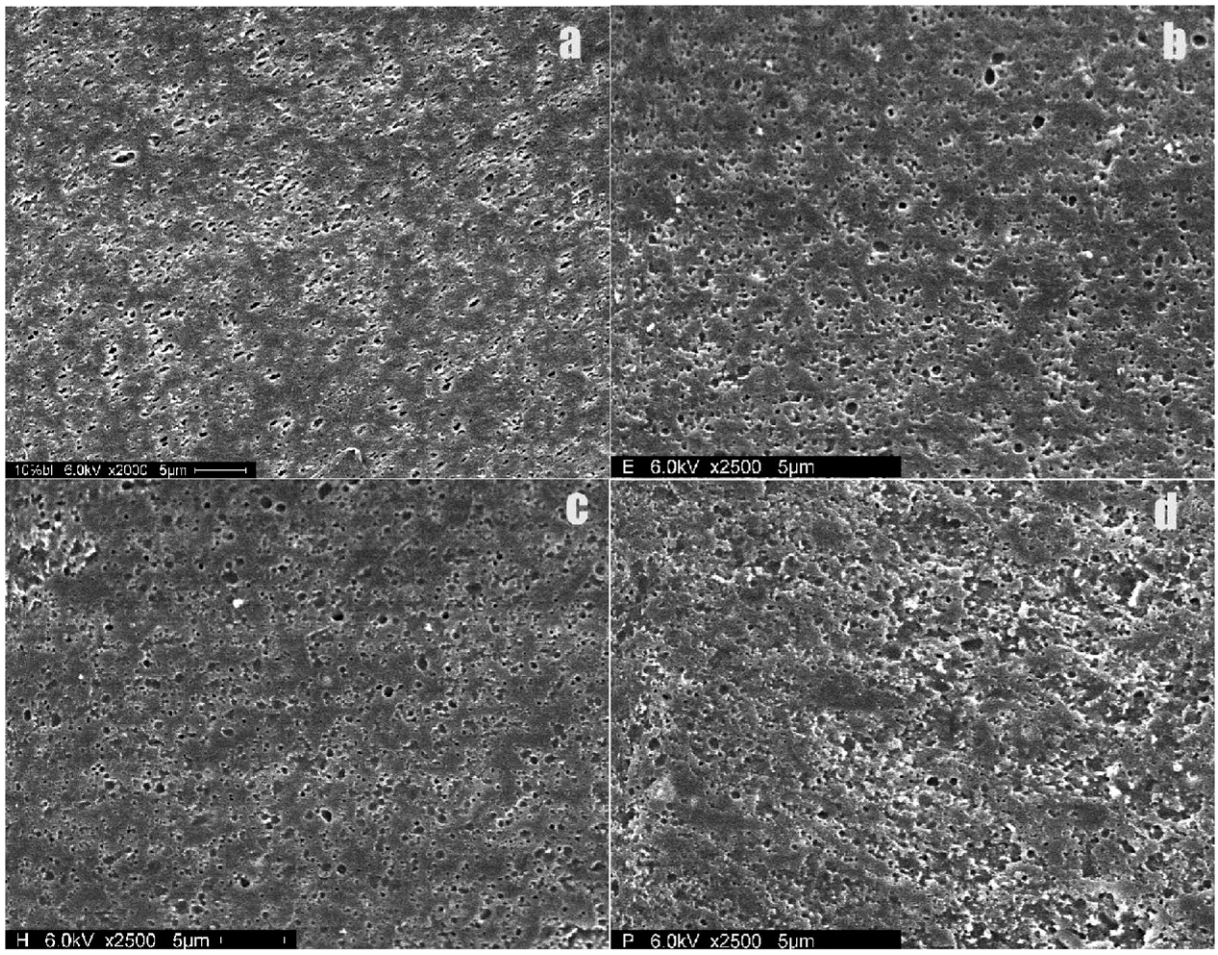

Fig. 2. Scanning electron microscope images of blend morphology, (a) PK_{90}-CSR_{10}; (b) PK_{80}-CSR_{20}; (c) $PK_{70}CSR_{30}$; (d) PK_{60}-CSR_{40}.

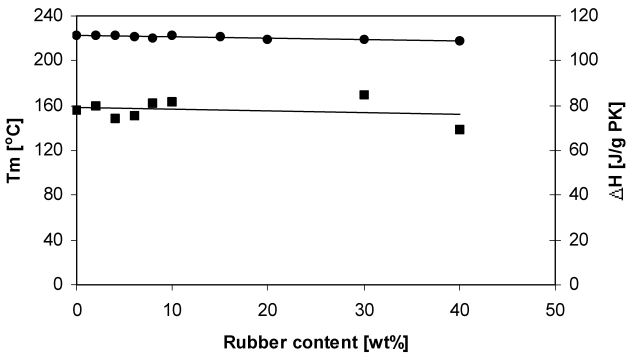

Fig. 3. Thermal properties as a function of rubber content, DSC 20 °C/min, ●, melting temperature; ■, melting enthalpy.

photo-diode placed on the other side of the specimen. Detection of cavitation by this method also has the advantage that strain rates in the impact regime can be applied.

3. Results

Blends were prepared from a polyketone terpolymer and a core shell rubber particles varying in composition from 0 to 40% wt PK-$_{90}$-CSR$_{10}$ will correspond to 90% matrix PK and 10% dispersed CSR phase.

3.1. Morphology

A critical parameter in the toughening process of blends is the morphology of the blend. It is now well accepted that the soft rubber phase should be present as fine particles, with a particle size less than 1 μm. However, very small particles, smaller than 0.05 μm, do not take part in the toughening process [25,40,41]. One of the requirements for obtaining a fine dispersion is that the interfacial tension between the polymer and the rubber phase is low. If the interfacial tension between the two phases is too high, one has to modify the interface, by adding an adhesion promoter or by chemically grafting the two phases. Another approach is of course the use of core-shell modifiers. With these modifiers the particle size is fixed. Core-shell materials are

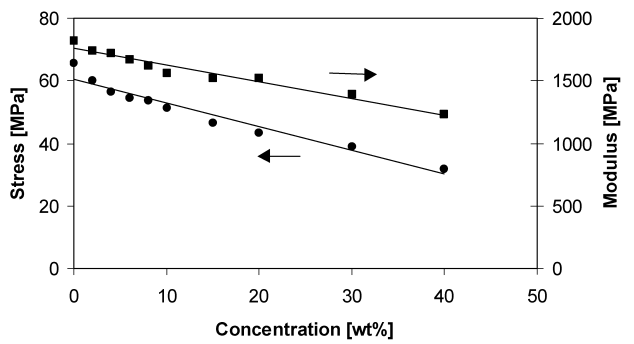

Fig. 4. Tensile modulus and yield stress as a function of rubber content for polyketone/rubber blends at 60 mm/min. ■, modulus; ●, yield stress.

supplied as agglomerates, and these clusters have to be broken up to disperse the rubber phase. The agglomerates may be broken up only partially and this will then effect the mechanical properties of the blend.

The morphology obtained for the blends with low rubber content were found to be of a fine dispersed phase in the matrix polymer (Fig. 2(a)). The obtained particle size was approximately 0.7 μm. The morphologies developed during extrusion and injection moulding show the core-shell modifier as a finely dispersed phase up to a rubber content of 40 wt% (Fig. 2(d)). There are no large agglomerates visible; the particles are dispersed homogeneously in the matrix polymer. The 40% blend has a somewhat rougher appearance, but this is mainly due to the larger content of CSR particles. The agglomerates are broken down to the small particles during extrusion, and the produced particle size is a result of breaking up and coalescence of particles. Larger rubber domains could cause the rubber toughening effect to be lower [27,39].

The morphology shown in Fig. 2 shows that the rubber particle size remains unaffected by the CSR content. The holes visible in the SEM pictures are of the same size for all blend compositions. The finely dispersed particles are more effective for toughening for reasons of stability. When voids are created by cavitation in the CSR phase the voids should not grow to a large size, otherwise a crack could be initiated and cause premature failure of the blend.

3.2. Thermal properties

The addition of soft rubber phase could influence the thermal properties of a polymer. The rubber particles may cause a change in micro-morphology of the polymer. The surface of the filler may act as a nucleating agent and thereby alter the amount or type of crystallinity. On the other hand, the polymer layer near the particle surface might have a reduced mobility and change the crystallisation rate. This can have a large influence on the bulk properties of the polymer system. It is known that the presence of small particles in polymers changes the spherulitical structure of the material. In blends, the common spherulitic structure of the crystalline phase is not visible, due to the large amount of crystallisation nuclei. For polypropylene, it has been shown [27] that the morphology changes from spherulitic to non-spherulitic did not change the melting temperature and the crystallinity. The different blend compositions were analysed with differential scanning calorimetry; the results are shown in Fig. 3.

The melting temperature remains unaffected by addition of a rubber phase, up to 40 wt% of rubber content the melting temperature is constant at 222 °C. The melting enthalpy of the polymer system is unchanged upon addition of a soft rubber phase. The melting enthalpy shows somewhat larger scatter than the melting temperatures but the effect of rubber phase on the melting enthalpy is negligible. The crystallinity calculated based on these data

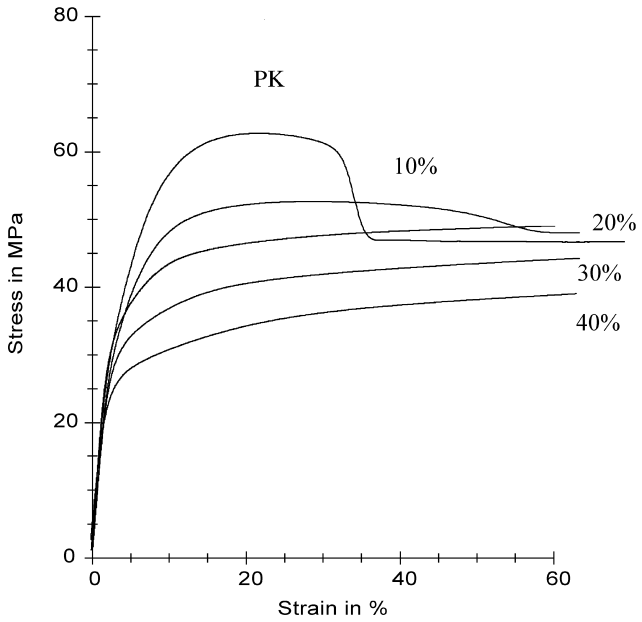

Fig. 5. Tensile engineering curves for blends with different rubber concentrations, 60 mm/min.

remained constant at 35 wt% (100% crystalline material ΔH : 227 J/g).

3.3. Tensile properties

The tensile modulus and yield stress as a function of rubber content are shown in Fig. 4.

The tensile strain rate used was $8.3 \times 10^{-4}\,s^{-1}$. The modulus and yield stress decreased almost linearly with increasing rubber content. The effect of rubber content is almost equal for the modulus and yield stress although these effects are described by entirely different models [4]. The decrease in modulus and yield stress is somewhat stronger than expected from the rule of mixtures for these blends.

The decrease in yield stress seems somewhat stronger than the decrease in modulus. This may have to do with the cavitation of the rubber spheres, which does not occur in the strain regime of the modulus. A remarkable feature of the tensile properties is the post-yield behaviour of the different blends. The rubber phase causes the post yield responds to be more stable.

Fig. 5 shows that the development of a neck does not occur at elevated rubber contents (>15 wt% rubber phase). The deformation is delocalised by the rubber phase. The localisation of deformation which leads to neck formation also causes the temperature of the specimen to rise locally. This is shown in Fig. 6, where the neck development and draw process are recorded with an infrared camera.

It is obvious from Fig. 6 that the homogeneity of deformation increases with rubber content. The formation of a neck is suppressed by the presence of a rubber phase, most likely due to the cavitation process and the consequent change in stress state at the particle size level. The strain softening is reduced with rubber content and therefore the local strain rate is reduced. The temperature development is also changed; this is caused by the decreased local strain rate and the smaller amount of matrix material that is plastically deformed. The maximum temperature of the sample was recorded with an infrared camera and the data is shown in Fig. 7.

The maximum temperature during deformation is clearly decreased with increasing rubber content. The polyketone terpolymer itself shows a ΔT of approximately 55 °C, while the 40% rubber blend shows a ΔT of 10 °C. This gives the rubber blend a more stable post yield behaviour, with much less strain softening. The fracture properties under impact conditions are therefore expected to be better.

3.4. Impact properties

The notched Izod impact strength for the different blend compositions as a function of temperature is shown in Fig. 8. The impact increases with temperature and shows a sharp increase in respect to the temperature, followed by a decrease. The impact strength at low temperatures is relatively low (5 kJ/m^2) and the fracture is macroscopically brittle. At elevated temperatures the fracture becomes ductile and the impact strength is very high (40–70 kJ/m^2). These high values are due to the shear yielding of the matrix polymer.

The brittle-to-ductile transition temperatures are clearly shifted below the glass transition of the matrix polymer which is around 15 °C. For the blends with larger rubber content (30–40 wt%) ductile fractures are found at temperatures as low as −40 °C (Fig. 9). This is quite

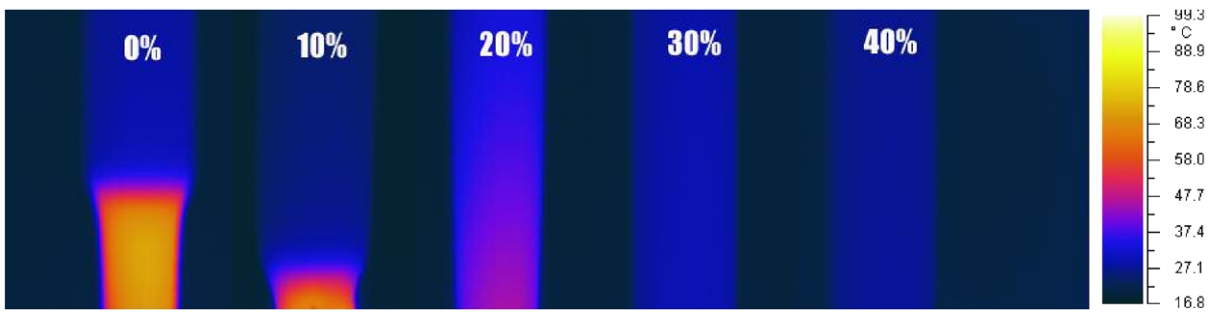

Fig. 6. Infrared images of different blends in tensile test at a strain rate of $8 \times 10^{-4}\,s^{-1}$.

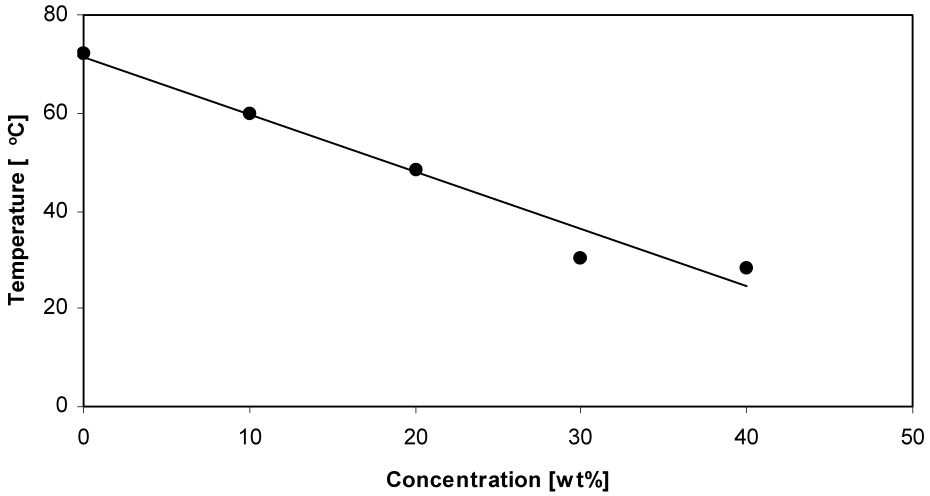

Fig. 7. Maximum temperature in tensile specimen as a function of rubber content, strain rate 8.3×10^{-4} s^{-1}.

remarkable since the terpolymer itself shows only ductile fractures above 90 °C. The highest rubber content did not show an improvement compared to the 30 wt% blend. This could be an indication that the melt stability has an effect on the mechanical properties.

An increase in rubber concentration causes a linear decrease in brittle-to-ductile transition temperature. At a certain level of rubber content the toughening effect is lowered. The dotted line indicated in Fig. 9 corresponds to the temperature region where the rubber phase starts to approach its T_g at these strain rates. The T_g of the rubber phase lies at −80 °C in a 1 Hz experiment, the strain rate at the crack tip is some decades higher and the T_g could be approached at temperatures around −50 °C under these impact circumstances. The toughening via cavitation of a soft phase could be hampered by the fact that the rubber stiffness is increased below the glass transition temperature (T_g). The shift of T_{bd} below this temperature is not possible, due to the prevention of the toughening micro-mechanism of rubber cavitation. This is also found for other semi-crystalline polymers such as nylon and polypropylene [27, 30].

3.5. Rubber cavitation process

The cavitation measurements have been performed on a Schenck hydropulse 25 VHS high speed hydraulic tensile tester The laser used was a helium–neon laser with a maximum output power of 30 mW and a wavelength of 633 nm. The data were sampled using a transient data recorder after which the data was transferred to a computer set-up. The test set-up is given in Fig. 2 and a typical plot of the resulting data is shown in Fig. 10. For this experiment test bars are used without a notch, the samples were 10 mm width and had a thickness of 4 mm. The piston displacement and initial clamp distance were used to calculate the strain.

The principle of the method is that cavitation in a blend is accompanied by a change in transparency due to stress

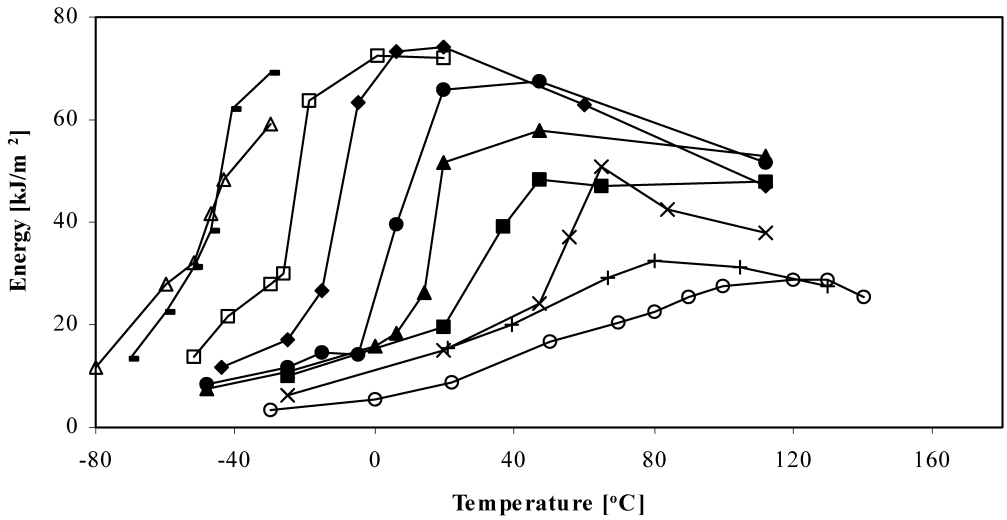

Fig. 8. Notched Izod impact results as a function of temperature for different blend compositions; ○ PK, + 2%, × 4%, ■ 6%, ▲ 8%, ● 10%, ◆ 15%, □ 20%, – 30%, △ 40%.

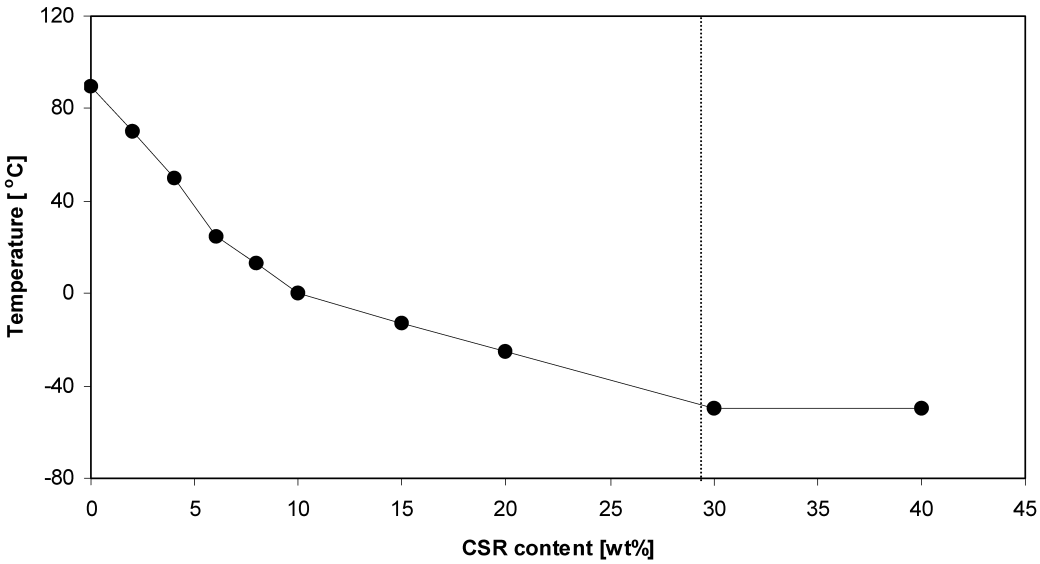

Fig. 9. Brittle to ductile transition temperatures as function of CSR content, notched Izod impact.

whitening. The stress whitening is caused by the scattering of the incident light by cavitated particles. When a strong light source is positioned on one side of the specimen, it is expected that at the onset of cavitation, the intensity of the transmitted light will drop suddenly. This lowering of the intensity of transmitted light can be detected by a photo-diode placed on the other side of the specimen. It will be clear that the cavitation stress as measured with this set-up is the stress acting on the blend when the rubber starts to cavitate. This stress is not the same as the stress acting on the rubber particles at the point of cavitation. The strain at the onset of cavitation is plotted versus rubber content in Fig. 11.

The yield strain is unaffected by the rubber content, the yield point is only dependant on the properties of the matrix polymer. The macroscopic cavitation strain remains constant at a value of 2.8%. The value is somewhat lower than has been found for nylon rubber blends by Dijkstra [30] et al., they have measured a cavitation strain of 4% with an identical experimental set-up for PA/BR blends. A constant cavitation strain implies a constant real cavitation stress. The macroscopic cavitation stress is plotted in Fig. 12 as a function of rubber content.

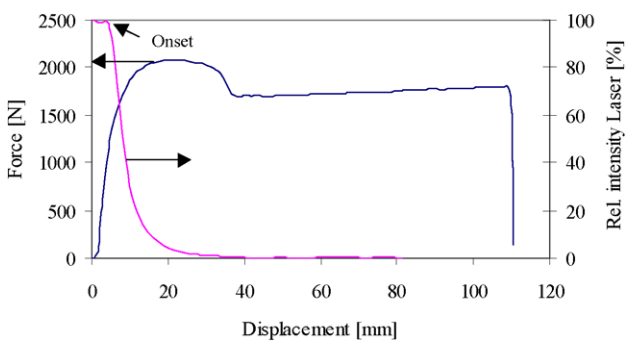

Fig. 10. Typical example of obtained result with laser intensity and tensile curve.

The yield stress decreases with rubber content as shown previously, the cavitation stress is also decreased with rubber content. This is mainly due to the decreased host matrix material with increasing rubber content. The rubber content seems to have little effect on the cavitation properties of the rubber phase.

3.6. Fracture deformation study

One of the striking aspects of the deformation behaviour of polymer/rubber blends is the occurrence of stress whitening in deformed samples When the fractured Izod samples are studied, stress whitening is visible in the region just ahead of the notch when the fracture type is brittle. When the specimen fails in a ductile manner, stress whitening can be seen over the entire fracture surface. The unnotched dumbbell shaped specimen, deformed in a tensile test, show stress whitening in the parallel section of the gauge. Stress whitening is linked to the ductile responds of the blend.

In the past, stress whitening in rubber toughened plastics was thought to be connected to crazing [42–44]. It was demonstrated by Rammsteiner [45] that stress whitening in rubber blends could be attributed to the cavitation of rubber particles. Gaymans et al. [40] showed that near the fracture surface the cavities were strongly deformed. Speroni and coworkers [46] demonstrated that at a larger distance from the fracture surface still voids were present, and that the deformation of these voids was a function of the distance to the fracture plane. Oostenbrink et al. [47] demonstrated that the deformation at high strain rates may be divided into three layers. At a large distance from the fracture surface a zone is visible where the particles are cavitated but the voids are not deformed. Closer to the fracture plane the voids

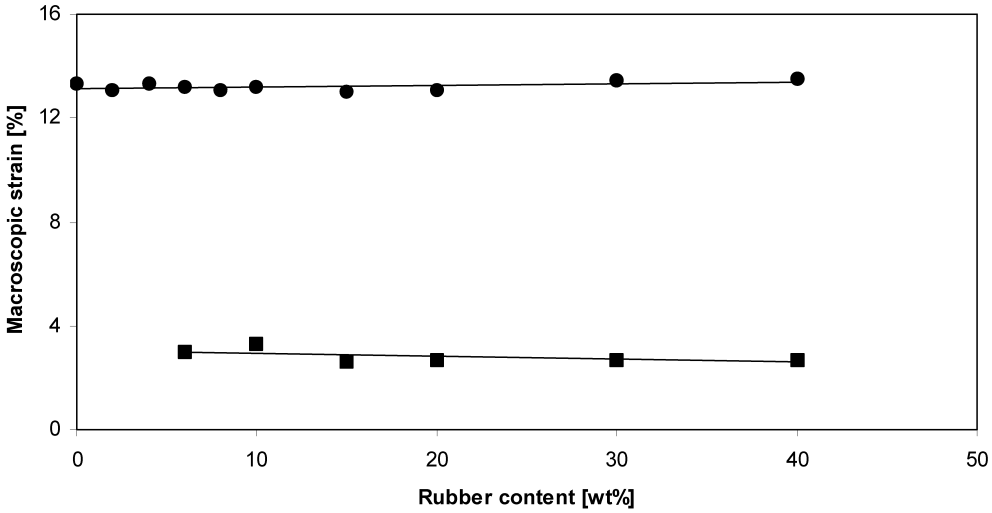

Fig. 11. Macroscopic cavitation strain and yield strain as a function of rubber content. ● Yield strain, ■ macroscopic cavitation strain.

become strongly deformed, and have ellipsoidal shapes. Directly beneath the fracture surface there is a third zone where no cavitation and deformation is visible. The authors suggest that local heating around the fast running crack tip is large enough to form a melt layer in the material. A similar effect has been reported by Boode [48], who found a practically undeformed layer beneath the fracture plane in ABS samples deformed in an Izod impact test.

If the relaxation layer is due to the local adiabatic heating, the samples deformed at a low strain rate should not show this relaxation layer. A scanning electron microscopy study was performed on deformed samples at low and high strain rates. Fig. 13 shows the deformation zone beneath the fracture surface for the low strain rate deformed polyketone rubber blend.

On straining of a blend, a stress concentration first develops around the modifier particles. In the second step, particle cavitation occurs. The voids then present in the material are elongated due to the deformation of the surrounding host matrix polymer. This fracture mechanism has been demonstrated by several authors [23,41,45–50].

It is clear from Fig. 13 that the cavities are present up to the fracture plane, the voids show strong deformation, this is seen in the stretch ratio of the cavities. The aspect ratio of the voids is a measure of the deformation strain of the matrix polymer next to the voids. The voids formed by cavitation are stable in the sense that they do not coalesce with each other. This is an important feature of the fracture mechanism; if the cavities grow to a too large size they could initiate early fracture of the material. The deformation is lowered if the distance to the fracture plane is increased. This is also shown in Fig. 14, the crack direction in this case was from right to left.

The deformation is lowered further down into the specimen. The voids due to cavitation of the modifier particles become more spherically shaped further down into the specimen. This indicates the lower orientation of the surrounding matrix polymer. There is no indication of a

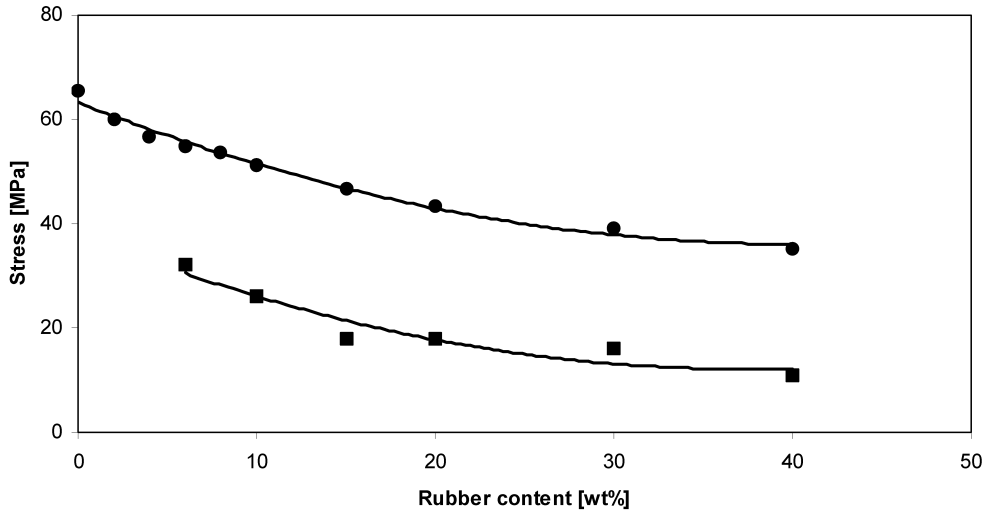

Fig. 12. Macroscopic cavitation stress and yield stress as a function of rubber content. ● Yield stress, ■ macroscopic cavitation stress.

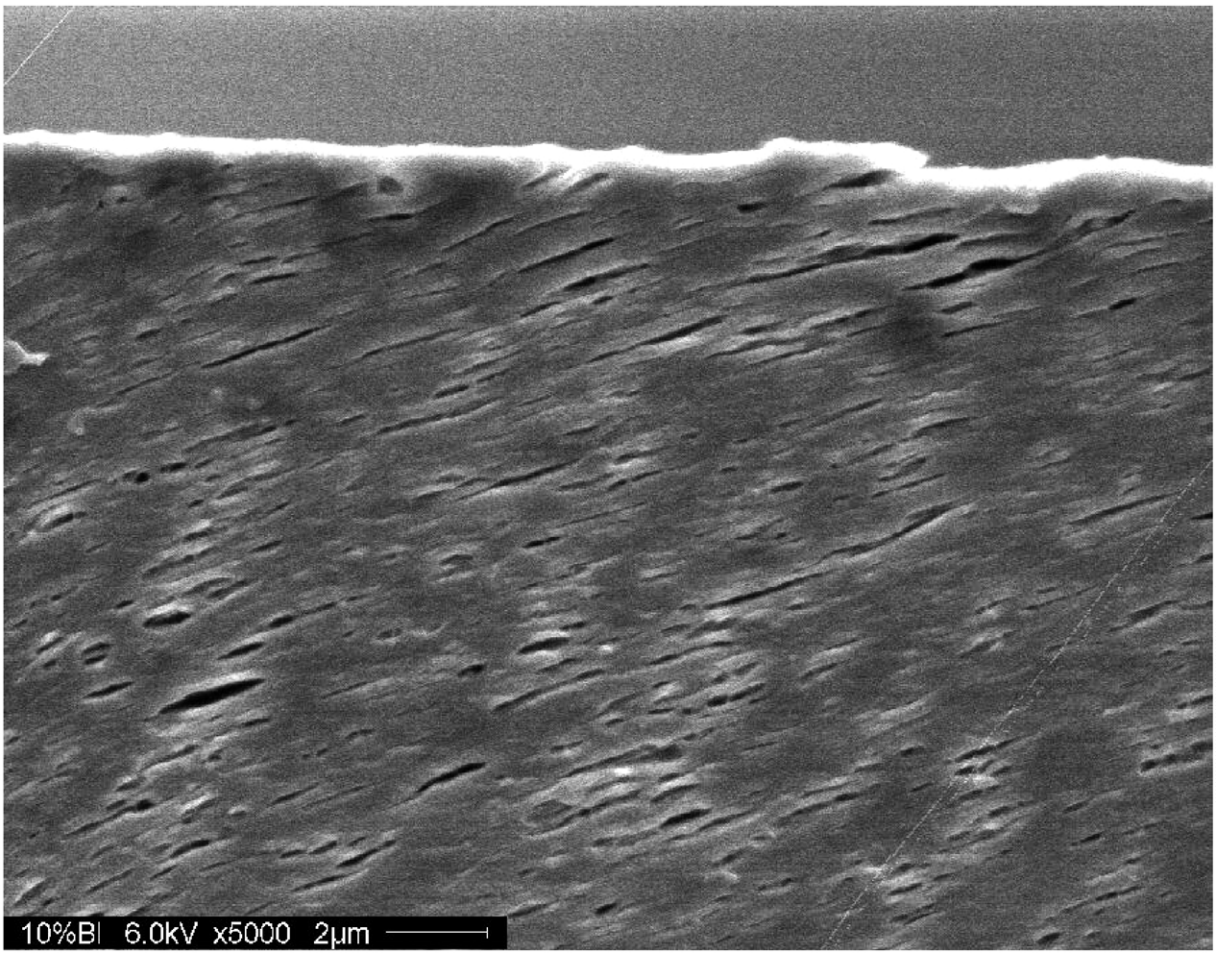

Fig. 13. Scanning electron microscope image of deformation zone beneath the fracture plane, (fracture was from left to right), low test speed, 10^{-3} m/s.

relaxed layer beneath the fracture surface. The temperature rise due to adiabatic heating is lower for these samples compared to the specimen fractured under impact conditions. The orientation of the formed cavities visible is due to the passing of the running crack. To demonstrate this more clearly a crack was arrested in a sample of a polyketone rubber blend. The crack was arrested, by a two-notch method. Two notches are milled into one specimen on opposite sides of the sample. The sample is then deformed in a tensile set-up. At both notches a crack is initiated, when one crack is propagated earlier/faster the second crack will stop due to the disappearing stress upon fracture of the first crack. This method resulted in an arrested crack, which was then consequently microtomed at −120 °C with a diamond knife and studied with scanning electron microscopy. Fig. 15 shows such samples.

The approaching crack deforms the particles and voids; the ellipsoidal shaped cavities are bend in the crack direction and create the characteristic orientated cigar shaped voids below the fracture surface. The strain reached is quite large, which is indicated by the high aspect ratio of the voids. The samples fractured at high strain rate were also studied with scanning electron microscopy (SEM). The typical deformation zones are shown in Fig. 16. Except for the relaxation zone found directly beneath the fracture plane, the structure of the deformation zone is quite similar to the structure found for specimen fractured at low strain rates.

The polyketone rubber blends show the same relaxation zone as found for other engineering materials such as nylon/rubber blends, Acrylonitrile-butadien-styrene (ABS) materials and polypropylene rubber blends [27,30,48]. This relaxation zone is related to the softening occurring at high deformation rates due to the adiabatic temperature rise of the material. The increase in temperature has been recorded with an infrared camera and temperatures are found up to 170 °C [28]. The relaxation layer has a size of approximately 20–30 μm. This is in good agreement with results found in previous studies, 3–5 μm for Polyamide-rubber blends [51] and 10–25 μm for Polypropylene-rubber blends [27]. The relaxation layer could be due to actual melting of the material, but it could also be sufficient that softening occurs and the elastic spring-back of the material causes the deformation to be reversed [52].

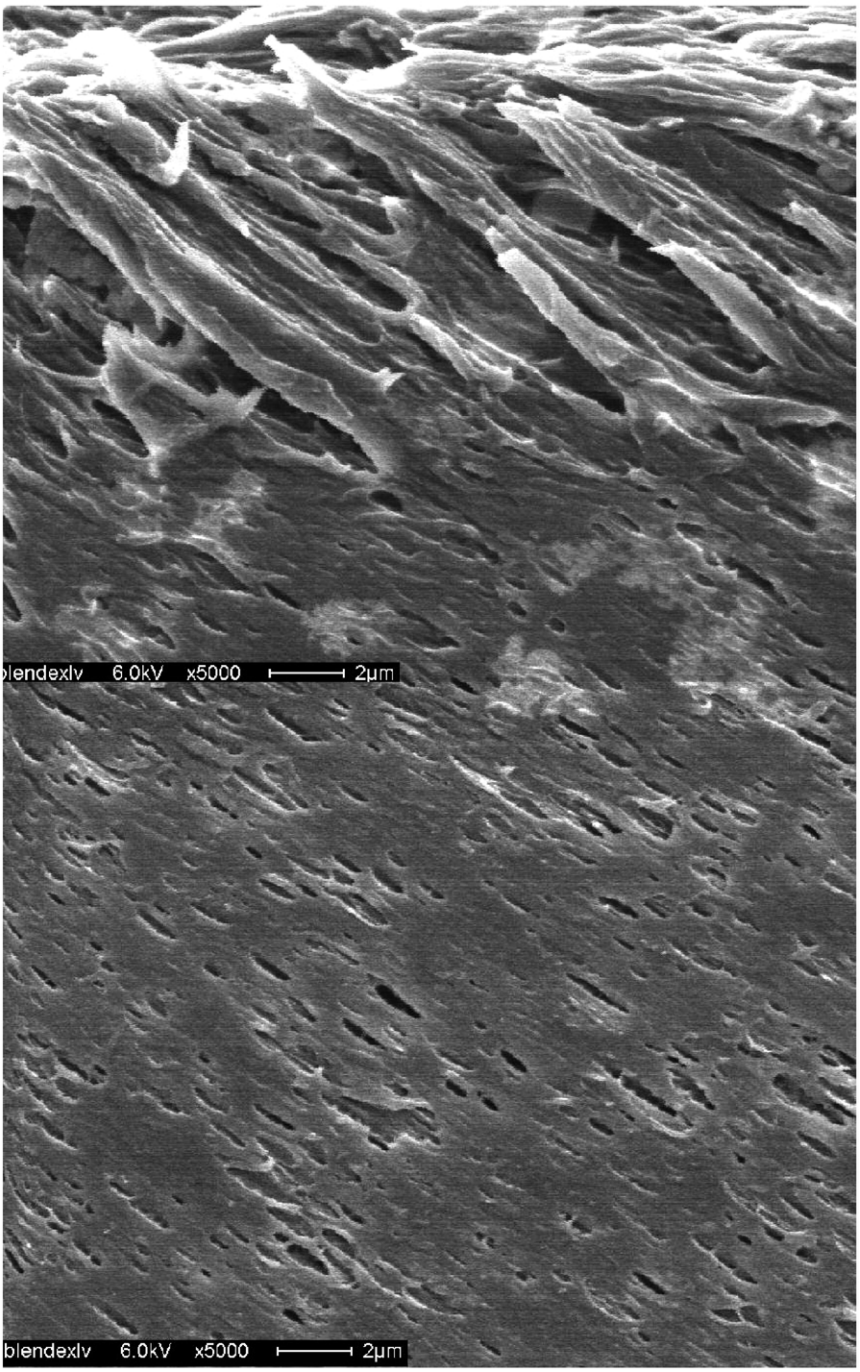

Fig. 14. Deformation of cavities beneath the fracture plane, scanning electron microscope image, samples deformed at low strain rate. (Fracture from right to left).

3.7. Infrared thermography

The discussed toughening mechanism of subsequent particle cavitation and shear yielding of the matrix polymer, involves stress concentration at the modifier particles during loading. One aspect of the influence of rubber content is the influence of stress field overlap at elevated rubber contents. It has been shown by Dijkstra et al. [30] that at a rubber content above 20% a slight decrease in cavitation strain was observed for nylon/rubber blends. This suggests that the cavitation stress on the rubber particles remains constant, the small decrease at higher rubber fractions is due to the stress field overlap, the strain necessary to reach the cavitation stress on the rubber particles is then reduced. To demonstrate how this process of stress field overlap may occur, a specimen was prepared with two milled in notches at opposite sides of the sample at an angle of 45°. This sample was then strained in a tensile set-up. The experiment

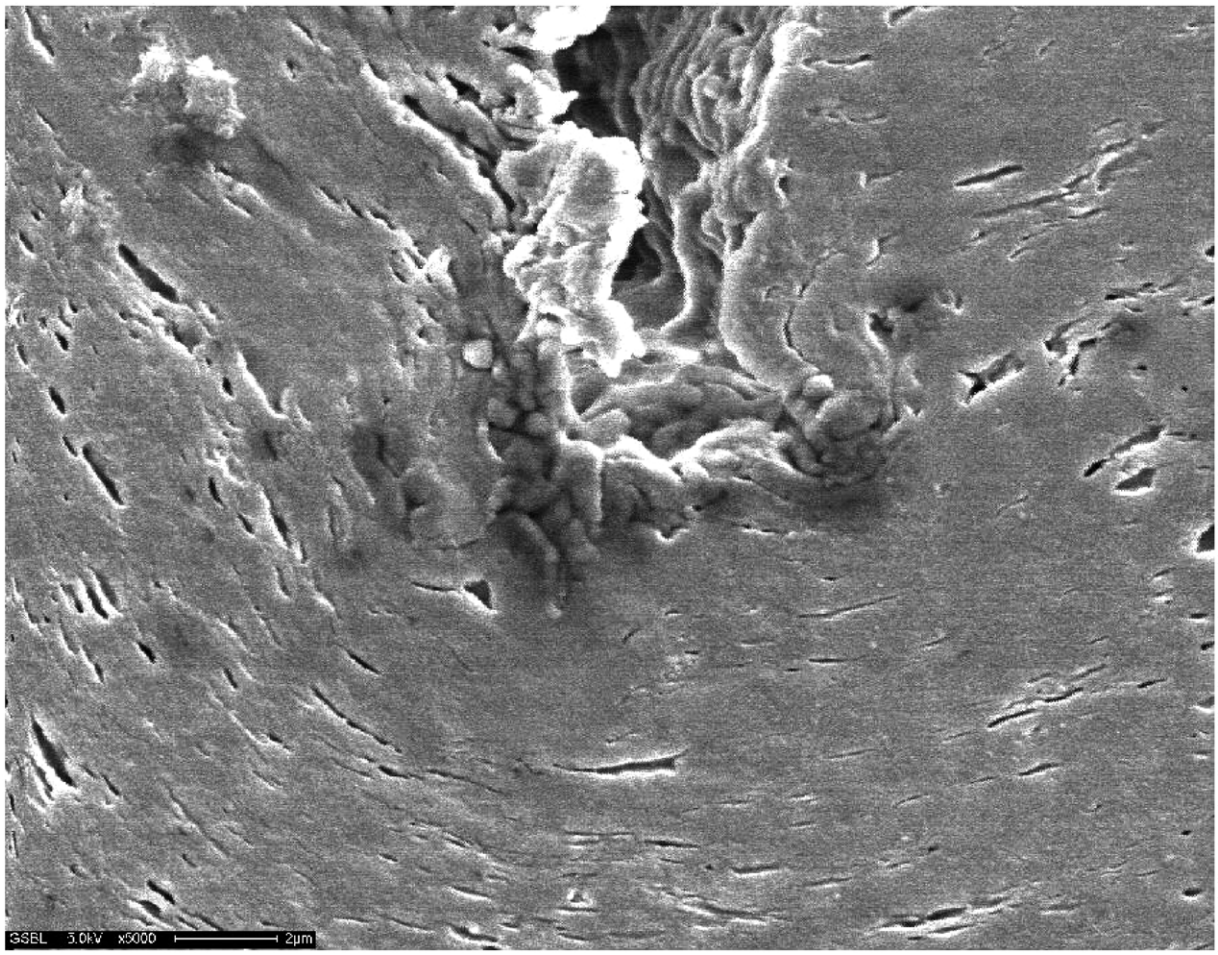

Fig. 15. Arrested crack in a polyketone/rubber blend.

was recorded with an infrared camera as described in Section 2. The plastic processes during deformation generate heat and warm up the material if the cooling rate lacks behind (i.e. adiabatic conditions). The temperature rises are indicative for the places within the sample where plastic deformation occurs. It is demonstrated in Fig. 17 that the stress fields around the two notches show overlap. The material shows clear shear bands at angles of 45° relative to the notch. The material in between the two notches shows larger deformation compared to the material on the outside of the notches. At the particle size level this process can occur in the same manner and thus show extensive stress field overlap at elevated rubber contents. The cavitation properties may be altered in such a case.

The effect of rubber content on the adiabatic heating of the material was determined for the dumbbell shaped specimen (see Section 3) as well as for the notched geometry. The temperature rise as a function of rubber content in a notched sample is shown in Fig. 18.

The polyketone terpolymer (0% blend) fractured in a brittle fashion, this is indicated by the small plastic zone size shown in Fig. 18. Upon addition of a soft elastomeric phase the plastic zone size increases considerably. Due to the more extensive plastic processes the heat generation is also increased. When the rubber content is increased the plastic zone size increases even further, the temperature reached in the specimen however, is not increased. This is due to the delocalisation of the plastic deformation. The local strain rate is lowered by the delocalisation of the plastic processes and consequently the temperature is lowered of the material during fracture. The amount of material, which is plastically deformed also, is lowered with increasing rubber content, this reduces the temperature development even further. The temperature of the plastic zone is plotted as a function of rubber content in Fig. 19.

The low temperature of the terpolymer (0% blend) is due to the macroscopic brittle responds of the polyketone. It was shown [28] for the unnotched experiments that the temperature of the polyketone terpolymer could rise up to 170 °C at a strain rate of 83 s^{-1}.

The plastic zone size decreases strongly with strain rate (Fig. 20), the large spherical shaped plastic zone at low strain rates transforms towards a line zone (dugdale line zone) at high strain rates. This indicates the extend to which the deformation localises upon increasing the loading rate.

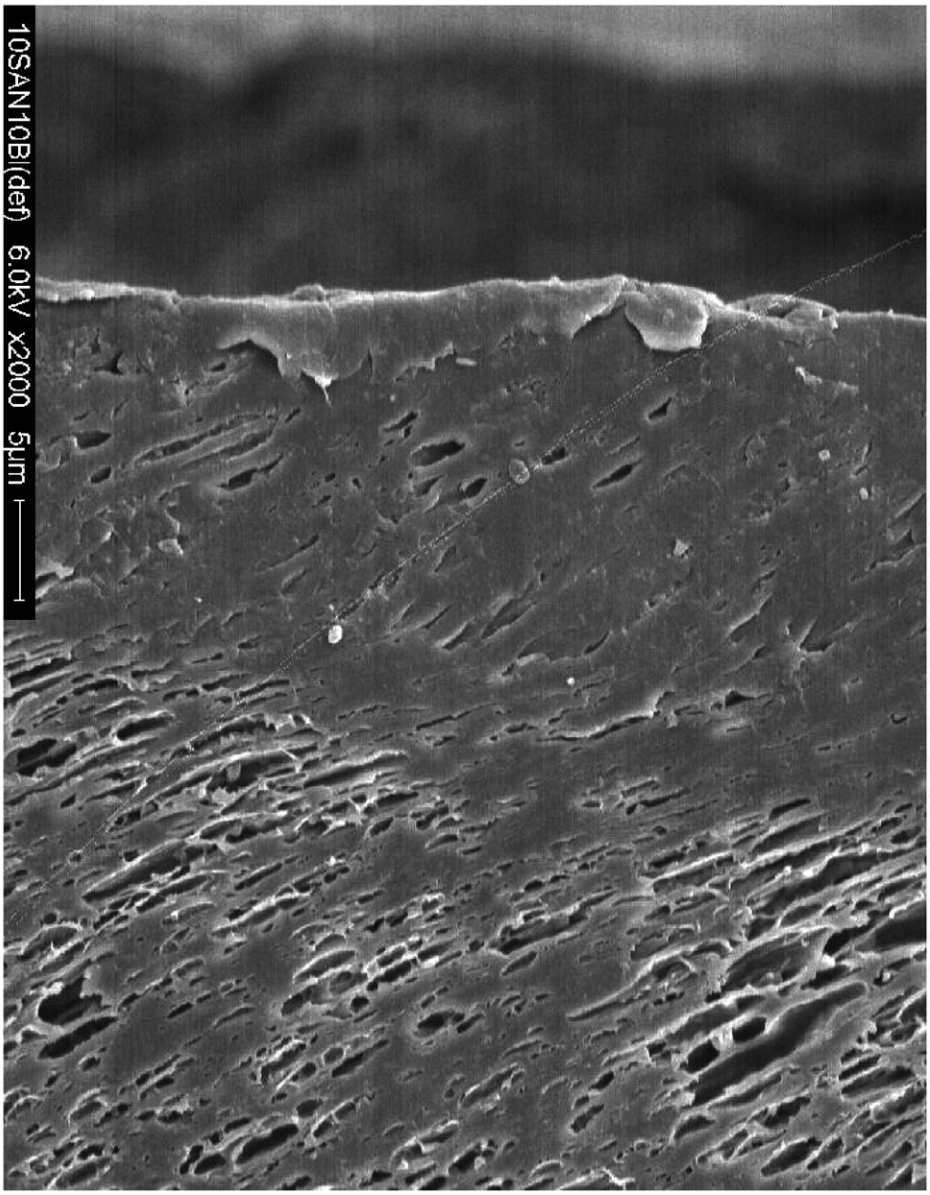

Fig. 16. Deformation zone beneath the fracture plane for polyketone rubber blend fractured at high strain rate.

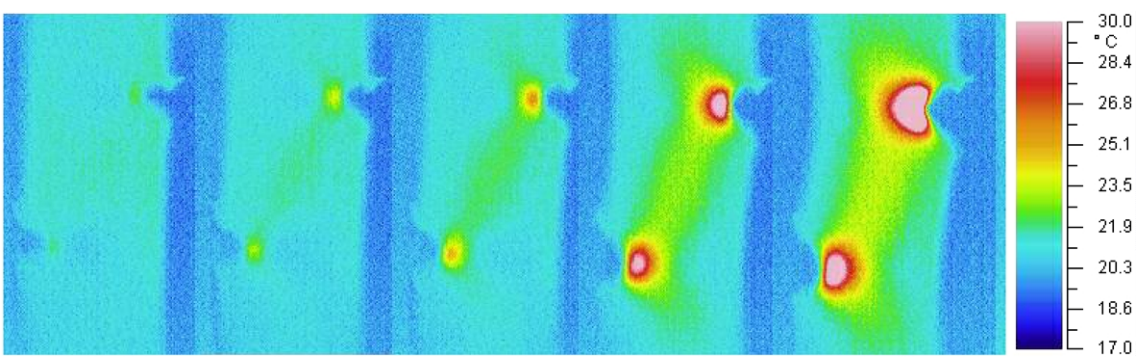

Fig. 17. Infrared thermographs of a double notched specimen under tensile loading at $8.3 \times 10^{-4}\ s^{-1}$.

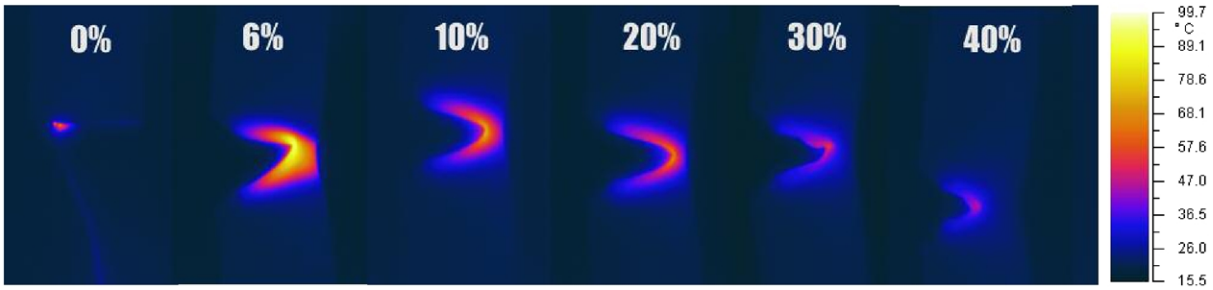

Fig. 18. Infrared images as function of rubber content, SENT, 20 °C, 10^{-3} m/s.

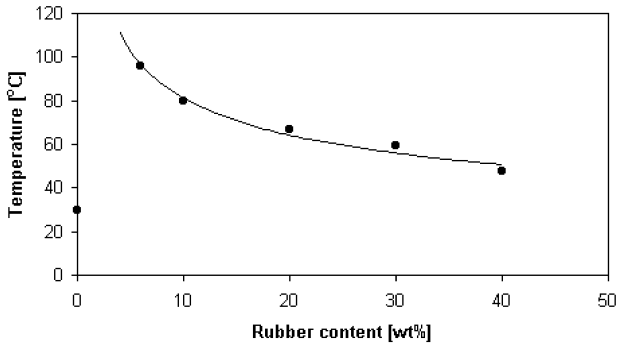

Fig. 19. Temperature of plastic zone as a function of rubber content, SENT, 20 °C, 10^{-3} m/s.

polyketone matrix very effectively, the brittle to ductile transition temperature was lowered from 90 to −40 °C with increasing rubber concentration (0–40 wt%). Cavitation experiments revealed that the macroscopic cavitation strain remained constant with increasing rubber content. A study of the deformation zone below the fracture surface showed that voids were produced by cavitation of the rubber phase. The voids were strongly deformed by the plastic deformation of the matrix polymer. At high strain rates a relaxation layer was found below the fracture surface, were the voids were no longer present. This relaxation zone was due to the adiabatic temperature rise of the material during fracture at high strain rates.

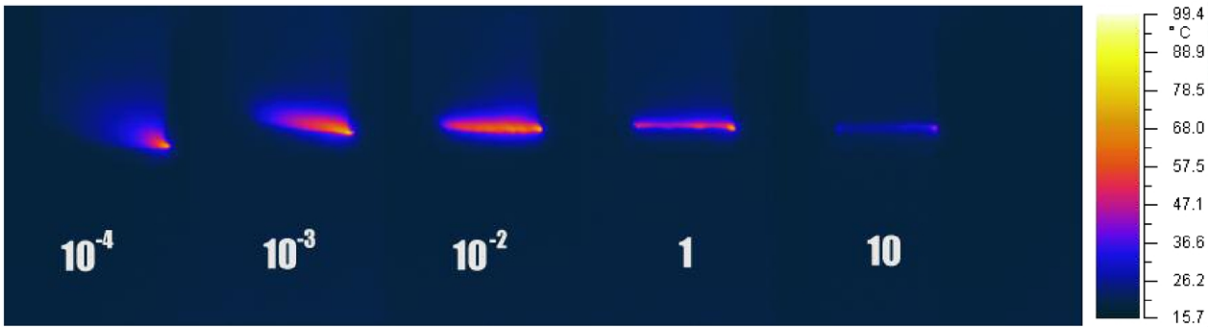

Fig. 20. Infrared thermograph of plastic zone size as function of strain rate, SENT, PK_{90}-CSR_{10}.

4. Conclusions

Blends of aliphatic polyketone terpolymer and a core-shell rubber were melt processed with varying CSR concentration of 0–40 wt%. The morphology obtained was of finely dispersed CSR particles in the polyketone matrix. The thermal properties of the matrix polymer remained unaffected by the addition of the CSR phase. The crystallinity was constant at 35 wt% and the melting temperature was not changed with rubber content. The tensile modulus and yield stress were decreased by the addition of the rubber phase to the aliphatic polyketone. The deformation was strongly delocalised with increasing CSR content. The temperature development during fracture was also strongly reduced with increasing rubber concentration. The CSR phase was found to toughen the aliphatic

References

[1] Drent et al. European Patent 121,965 (SHELL); 1984.
[2] Kunstoffe, 88, 8,1158; 1998.
[3] Zuiderduin WCJ, Huétink J, Gaymans RJ. J Appl Polym Sci 2003;91:2558.
[4] Bucknall CB. Adv Polym Sci 1978;27:121.
[5] Donald AM, Kramer EJ. J Mater Sci 1982;17:1765.
[6] Yee AF, Pearson RA. J Mater Sci 1986;21:2462.
[7] Dijkstra K, Van der Wal A, Gaymans RJ. J Mater Sci 1994;29:3489.
[8] Gaymans RJ. Toughening of semi-crystalline thermoplastics, polymer blends. Performance, vol. 2. New York: Wiley; 2000.
[9] Walker A, Collyer A. Rubber toughening mechanisms in polymeric materials, rubber toughening of engineering plastics. London: Chapman & Hall; 1994.
[10] Ayre DS, Bucknall CB. Polymer 1998;39:4785.
[11] Paul DR, Bucknall CB. Polymer blends. Performance, vol. 2. New York: Wiley; 2000.

[12] Lutz JT, Dunkelberger DL. Impact modifiers for PVC, the history and practice. New York: Wiley; 1992.
[13] Cruz-Ramos CA. Core-shell impact modifiers, polymer blends. Performance, vol. 2. New York: Wiley; 2000.
[14] Penco M, Pastorino MA, Occhiello E, Garbassi F, Braglia R, Giannotta G. J Appl Polym Sci 1995;57:329.
[15] Borggreve RJM, Gaymans RJ, Eichenwald HM. Polymer 1989;30:78.
[16] Karger-Kocsis J, Kalló A, Szafner A, Bodor G, Sényei Z. Polymer 1979;20:37.
[17] Martuscelli E, Silvestre C, Abate G. Polymer 1982;23:229.
[18] Chou CJ, Vijayan K, Kirby D, Hiltner A, Baer E. J Mater Sci 1988;23: 2521.
[19] Púkansky B, Tüdös F, Kalló A, Bodor G. Polymer 1989;30:1399.
[20] Jang BZ, Uhlmann DR, vander Sande JB. J Appl Polym Sci 1984;29: 4377.
[21] Danesi S, Porter RS. Polymer 1978;19:448.
[22] Becu L, Maazouz A, Sautereau H, Gerard JF. J Appl Polym Sci 1997; 65:2419.
[23] Muratoglu OK, Argon AS, Cohen RE, Weinberg M. Polymer 1995; 36:4771.
[24] Chang FC, Hsu HC. J Appl Polym Sci 1993;47:2195.
[25] Oshinski AJ, Keskkula H, Paul DR. Polymer 1992;33:268.
[26] Kinloch AJ, Yuen ML, Jenkins SD. J Mater Sci 1994;29:3781.
[27] van der Wal A, Gaymans RJ. Polymer 1999;40:6067.
[28] Zuiderduin WCJ. Deformation and fracture of aliphatic polyketones. Thesis. University of Twente; 2002, ISBN 90-365-17656.
[29] Borggreve RJM, Gaymans RJ, Schuijer J, Ingen Housz JF. Polymer 1987;28:1489.
[30] Dijkstra K. Deformation and fracture of nylon 6-rubber blends. Thesis. University of Twente; 1993.
[31] Kayano Y, Keskkula H, Paul DR. Polymer 1996;37:4505.
[32] Gaymans RJ, van der Werf JW. Polymer 1994;35:3658.
[33] Lu M, Keskkula H, Paul DR. J Appl Polym Sci 1996;59:1467.
[34] Lageron JM, Vickers ME, Powell AK, Davidson NS. Polymer 2000; 41:3011.
[35] Waddon AJ, Karttunen NR. Polymer 2001;42:2039.
[36] Stadlbauer M, Eder G, Janeschitz-Kriegl H. Polymer 2001;42:3809.
[37] Zuiderduin WCJ, Homminga DS, Huétink J, Gaymans RJ. Polymer 2003;44:6361.
[38] Struik LCE. Physical aging in amorphous polymers and other materials. Amsterdam: Elsevier; 1978.
[39] Way JL, Atkinson JR, Nutting J. J Mater Sci 1974;9:293.
[40] Gaymans RJ, Borggreve RJM, Oostenbrink AJ. Makromol Chem 1990;38:125.
[41] Oshinski AJ, Keskkula H, Paul DR. Polymer 1996;37:4919.
[42] Lazzeri A. PhD Thesis. Cranfield Institute of Technology, UK; 1991.
[43] Bucknall CB. Toughend plastics. London: Applied Science Publishers; 1977.
[44] Cimmino S, Coppola F, d'Orazio L, Greco R, Maglio G, Malinconico M, Mancarella C, Martuscelli E, Ragosta G. Polymer 1986;27:1874.
[45] Ramsteiner F, Heckmann W. Polym Commun 1985;26:199.
[46] Speroni F, Castoldi E, Fabbri P, Casiraghi T. J Mater Sci 1989;24: 2165.
[47] Oostenbrink AJ, Dijkstra K, vander Wal A, Gaymans RJ. PRI conf Cambridge, paper 50, 1990.
[48] Boode JW, Gaalman AEH, Pijpers AJ, Borggreve RJM. Poster presented at the Prague Macromol Meetings; 1990.
[49] Oshinski AJ, Keskkula H, Paul DR. J Appl Polym Sci 1995;58:1175.
[50] Kim GM, Michler GH, Gahleitner M, Fiebig J. J Appl Polym Sci 1990;60:1391.
[51] Janik H, Gaymans RJ, Dijkstra K. Polymer 1995;36:4203.
[52] Dijkstra PTS, Gaymans RJ, Van Dijk DJ, Huétink J. Polym Engng Sci 2003;43:1613.